Leaky wave enhanced feed arrays for the improvement of the edge of coverage gain in multibeam reflector antennas

Leaky Wave Enhanced Feed Arrays for the Improvement of the Edge of Coverage Gain in Multibeam Reflector Antennas

Nuria Llombart, *Member, IEEE*, Andrea Neto, *Member, IEEE*, Giampiero Gerini, *Senior Member, IEEE*, Magnus Bonnedal, *Member, IEEE*, and Peter De Maagt, *Fellow, IEEE*

***Abstract*—The performance of multibeam focal plane arrays feeding a single aperture is usually reduced due to conflicting requirements on the feed elements. Dense packing is usually required to minimize the beam separation, while typically large feed apertures are needed to provide the high feed directivity to reduce spillover losses from the reflector. In this paper the use of dielectric super-layers to shape the radiation pattern of each feed is demonstrated. The shaping is obtained by exciting, according to design, a pair of TE/TM leaky waves. The spillover from the reflector is reduced without physically increasing the dimensions of each single element aperture. A prototype of a feed array composed of 19 waveguides arranged in a hexagonal lattice was designed, manufactured and tested. The measured embedded patterns provided an increase of the edge of coverage gain, with respect to the free space case, of at least 0.6 dB in an operating bandwidth (BW) of $\approx$ 12%. Moreover when reactive loading of adjacent feeds is adopted the increase in the edge of coverage with respect to the free space case was demonstrated to be larger than 1.6 dB over a 3% BW.**

***Index Terms*—Leaky wave antennas, leaky waves, reflector antenna feeds, reflector antennas.**

I. Introduction

PRESENT and next generation satellite telecommunication systems often require multiple beam capability. In particular Ka band multibeam down links are being used to achieve efficient coverage of the earth and continents. The three fundamental ways to achieve high coverage gain are overlapping feed arrays with sophisticated feed networks, interleaved beams with multiple apertures (typically 4 reflector), and a single aperture with a single feed per beam designs [1]. This last approach is clearly much less expensive to implement, however it suffers from reduced performance.

Manuscript received July 3, 2007; revised December 17, 2007.

N. Llombart was with the Netherlands Organization of Applied Scientific Research (TNO), Den Haag 2597 AK, The Netherlands. She is now with the S.W.A.T. Group, Jet Propulsion Laboratory, California Institute of Technology, Pasadena, CA 91109 USA (e-mail: nuria.llombartjuan@tno.nl).

A. Neto is with the Netherlands Organization of Applied Scientific Research (TNO), Den Haag 2597 AK, The Netherlands (e-mail: andrea.neto@tno.nl).

G. Gerini is with the Netherlands Organization of Applied Scientific Research (TNO), Den Haag 2597 AK, The Netherlands (e-mail: giampiero.gerini@tno.nl).

M. Bonnedal is with Saab Ericsson Space, Gothenburg, Sweden (e-mail: magnus.bonnedal@space.se).

P. De Maagt is with the Electromagnetics Division, European Space Agency, 2200 AG, Noordwijk, The Netherlands (e-mail: Peter.de.Maagt@esa.int).

Color versions of one or more of the figures in this paper are available online at http://ieeexplore.ieee.org.

Digital Object Identifier 10.1109/TAP.2008.922680

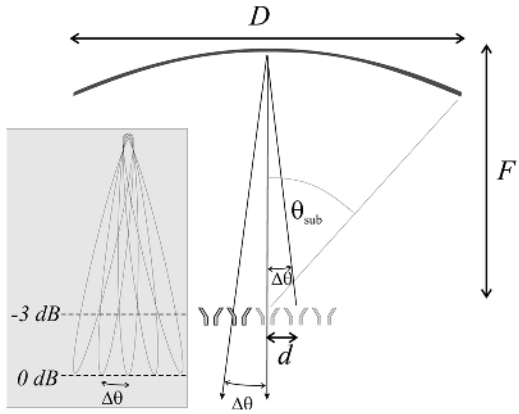

Fig. 1. Schematic view of a multibeam reflector system.

A. General Problem With the Single Feed Per Beam Design

Let us consider a generic array aimed at generating multiple independent beams, separated by a given angle $\Delta\theta$. The array is assumed to be in the focal plane of a reflector system as in Fig. 1. The basic parameters characterizing such a multibeam system are: the beam separation $\Delta\theta$, the reflector diameter, D, and the focal distance, F. These three parameters always define a sampling rule for the focal plane array depending on the desired beam properties and cross over between the beams. As an example, a first order dimensioning could be based on the assumption that the reflector is uniformly illuminated and that, at the cross over between two adjacent beams, the roll-off (field drop with respect to beam peak) is -3 dB. In this case (see Appendix) the basic sampling rule is

$$d \approx (F/D)\lambda_0 \tag{1}$$

where λ_0 is the wavelength at the central operating frequency, f_0. All the power that is launched by the feed but that is not intercepted by the reflector is effectively lost for the system (spillover). In order to enhance the spillover efficiency one would like to use large, more directive feeds. But (1) suggests that the dimensions of the apertures are limited by the period. As a rule of thumb, the radiation patterns ($|E|^2$) from standard feeds, e.g., horns, can approximately be modelled as $\cos^q(\theta)$, where q depends on the feed type and aperture size. Simplified

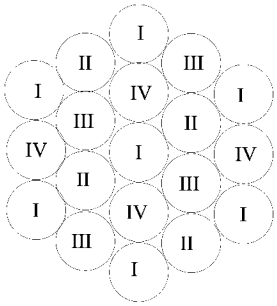

Fig. 2. x 4 reuse scheme. Frequency and/or polarization re-use schemes are possible.

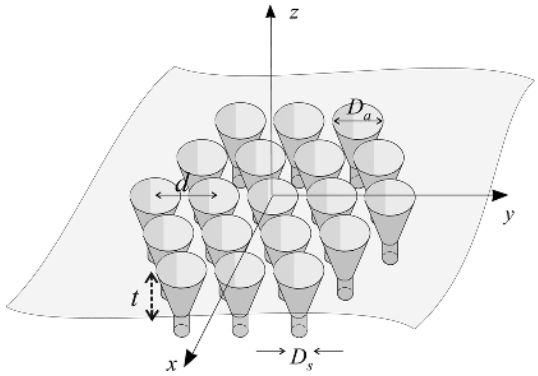

Fig. 3. Hexagonal grid array with periodicity d of circular metallic waveguide D, here the array is drawn opening in a infinitely extended ground plane. The apertures fully sample the array.

formulas to evaluate the q parameter for standard horns are given in [12]. The spillover efficiency associated to center fed reflectors can be approximated as $\eta_{\rm so} = 1 - \cos^{q+1}(\theta_{\rm sub})$. As shown in Fig. 1 F/D also defines the subtended angle $\theta_{\rm sub}$. As a relevant example, an aperture of $\lambda_0 \cdot \lambda_0$ roughly corresponds to $q = 5$, which for $\theta_{\rm sub} = 30^\circ$ corresponds to losses in spillover of 2.4 dB.

Equivalent conclusions would hold for any reflector illumination and beam overlap configurations: spillover is the limiting factor for a full field of view. For this basic reason, as also discussed in [1], the single feed per beam approach is usually not adopted for telecommunication satellite systems. This paper proposes an improvement that could make this single feed per beam option viable and would significantly reduce the costs of multibeam systems.

B. Leaky Wave Enhancements of Antenna Performances

G. V. Trentini [2] was the first to propose the use of a partially reflecting screen to increase the directivity of a single aperture. A point source would generate an ensemble of waves that impinge on a screen that is partially reflective and partially transmitting. The reflected rays propagate laterally and then are redirected towards a partially reflecting screen, so that they generate a unique wave that mainly radiates in the broadside direction. Since then this technique has been proposed in many different variations that involve periodic super-layers realized in dielectric or metal materials [3]–[6]. In [7] the fact that the enhancement in gain is due to the excitation of leaky waves has been clarified. Most recently, [8] studied the compromise between bandwidth and directivity for printed antennas and arrays in the presence of periodic super-layers.

In [9], leaky waves were also used to enhance the radiation performance of small antennas. The emphasis was, contrary to other works, not on the increase of the directivity of the source, but on the shaping of the pattern. In fact the target was to optimize the gain of the overall system composed by a feed + reflector and not the source alone. In [9] both taper and spillover efficiencies were improved choosing centrally fed reflectors as an example. In a p-feed demonstrator, an operational bandwidth of 10% was achieved for the antenna system.

In this paper, the design of multibeam focal plane arrays using an overlapped feed concept realized via dielectric super-layers is discussed. The results of [10] are used as starting point. In fact in [10], after a discussion on the impact of mutual coupling on overlapped feeds configurations, a specific radiator design was presented.

C. Structure of the Paper

The structure of the paper is as follows. First a short introduction on the use of focal plane multibeam systems is provided with the parameters characterizing the properties of such systems and in particular the edge of coverage (EoC) gain. A reuse scheme is considered to maximize the isolation of neighboring beams. The performance of a standard array configuration operating in free space (without superstructures to create overlapping between feeds) is used as reference. Then a first system design, indicated as resistively loaded design, is described. The proposed structure was manufactured and measured showing a moderate gain enhancement, with respect to the reference, over 12% bandwidth (BW). For moderate operational BW, higher EoC gain enhancement with respect to reference can be obtained by reactively loading the neighboring waveguides. A second prototype demonstrator was manufactured to explicitly demonstrate this aspect. The relation between the design methodology described in this paper and the Stein's Limit, [18], [19] is discussed just before the conclusions.

II. System Parameters and Formulation of the Problem

In this section the requirements are first given and explained, then the performances realized with a standard reference array are described in order to establish a benchmark for a comparison with leaky wave enhanced feeds that will follow in the next sections.

A. System Requirements

The specific telecom scenario that is considered will be that of satellite based down-link in Ka band. The area to be covered by independent beams is arranged in an hexagonal lattice with beam separation $\Delta\theta \approx 1^\circ$. Correspondingly, an hexagonal array is placed in the focal plane of a reflector system. Moreover, a reuse scheme (x4) will be used in order to achieve a maximal isolation between the neighboring channels (beams). The implementation of the interleaved beams and of the single aperture corresponding focal plane array is based on the scheme

described in Fig. 2. As will be discussed in the next sections the scheme can be implemented simply by a x4 frequency reuse or by a mixed frequency and polarization reuse. It can be anticipated that the reflector system will be an offset fed Gregorian in order to minimize the blockage of the direct radiation by a large feed array. The array elements are assumed circularly polarized in order to maintain the highest applicability. Finally, the bandwidth is required to be at least 6% which encompasses many applications. While in standard multibeam systems the F/D of the reflector is often a parameter that can be used for system optimization, in leaky wave enhanced feed systems, the F/D is mostly dependent on the target bandwidth. Thus, if the BW is a requirement, the F/D is already fixed in a certain range. For instance, as was clarified in [9] and [10], a BW of 6% for the impedance or the mutual coupling approximately corresponds to leaky waves pointing towards 15° from broadside. Consequently, the reflector half angle,$\theta_{\rm sub}$, which needs to be optimized can be anticipated to be in range from 25° to 40°, corresponding to an F/D in the range 1.2-0.8. Such a moderate F/D ratio limits the scanning performance of the antenna system. However the limited scanning should not be seen as a definitive limit. A smaller bandwidth could have allowed the selection of a super-layer that supported leaky waves pointing to smaller angles from broadside so that overall the definition of systems with F/D significantly larger would have been possible. This study aims at providing general design guidelines, which can then be tuned to the more specific needs of an engineer.

B. A Reference Array

A standard waveguide array, whose geometry is described in Fig. 3, is investigated. An hexagonal grid array is chosen with periodicity, d, set to 1.2 λ_0. Such an array is suitable to feed reflector systems characterized by relatively small F/D ratios $(F/D \approx 1)$, comparable with the ones anticipated for the leaky wave enhanced feeds.

The array consists of 19 circular waveguide horns that open in an finite ground plane of dimensions $(12\lambda_0 \cdot 12\lambda_0)$. The reference system has the z axis normal to the ground plane. The circular apertures are obtained by flaring the feeding waveguides of diameter $0.7\lambda_0$ to a diameter of $1.1\lambda_0$, over a taper of length $t = \lambda_0$. With this arrangement the apertures cover almost the entire central part of the ground plane. The reflection coefficients, S_{ii} parameters, of each of the waveguides are lower than -23 dB's and the mutual coupling coefficients, S_{ij} are lower than -30 dBs over the entire operational BW.

C. Edge of Coverage Gain and Other Performance Parameters

The use a dual reflector system is proposed. The scanning impairment due to the offset is reduced using the Mizucuchi's condition [13] which conserves the optical symmetry of a center fed reflector system. Also the sub-reflector magnification can be used to match the feed subtended angle (and hence spillover) to the main reflector F/D ratio. The geometry of the system is shown in Fig. 4 and the nominal dimensions are reported in Table I (the reflector system is assumed to be in X band, representing a 2.8 times scaled version of the Ka one). As a starting point the design of the system was still based on the equivalent

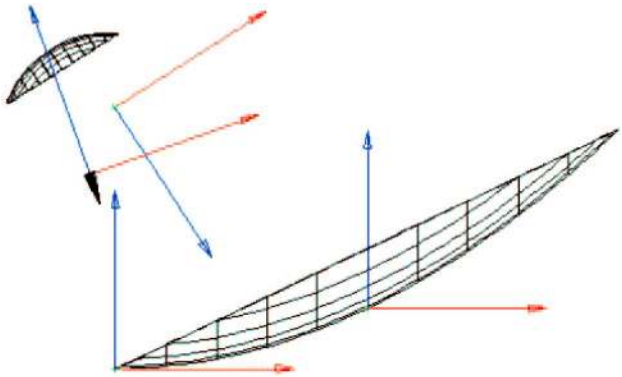

Fig. 4. Schematic view of a Gregorian dual offset reflector configuration.

TABLE I
REFLECTOR SYSTEM NOMINAL DIMENSIONS

Parameter	Value	Unit
Main reflector focal distance	1.1	m
Nominal reflector diameter	2.1	m
Main aperture center offset	1.056	m
Sub reflector magnification	1.9	-
Sub reflector focal to focal distance	0.3	m
Angle of sub reflector axis to main axis	21	deg
Feed angle referred to sub reflector axis	13.17	deg
Extended sub reflector diameter	10	%

diameter D and focal distance F using the equivalent paraboloid concept, [12].

To accurately evaluate the performances of a reflector system fed by the reference array in Fig. 3, the far fields of the reflector need to be calculated. The fields radiated by the reference array, calculated using Microwave Studio CST [15], have been used as inputs to calculate the secondary fields via the Physical Optics code GRASP, [14].

The key merit parameter for these multibeam systems is the edge of coverage, EoC, gain, which in the hexagonal lattice is defined at the cross over between three adjacent beams: $G_{\rm eoc} = G(\Delta\theta/\sqrt{3})$. Fig. 5 shows the EoC gain calculated from the radiation patterns predicted by the reference array in Section II.B, for a reflector that provides $\Delta\theta \approx 1°$, which, given the array spacing of $1.2\lambda_0$, corresponds to $F = 67\lambda_0$. The EoC gain is shown as a function of the normalized frequency and for different F/D, since the F/D ratio was the main design parameter in order to find the maximum EoC gain. The optimum F/D ratio was found to be around 0.85. Another optimization parameter was the feed axial position, corresponding to finding the optimum phase center. In the optimum case the roll-off at the edge of coverage and at the central frequency (10 GHz) is -5.46 dB. The relevant 10 GHz patterns are shown in Fig. 6.

Table II shows the most important parameters characterizing the secondary beams from each of the feeds in the reference multibeam array, for $\mathrm{F/D} = 0.85$. Note that the roll-off is also evaluated at the EoC. Adopting a reuse scheme of 4x, assumed to be realized via frequency switching, the isolation is the maximum overlap between beams located at two beam-separations, Fig. 6. The obtained isolation is around 15 dB which can be marginal in some applications. A reuse scheme of at least 7x will, however, provide a beam isolation of well below 20 dB.

TABLE II
PARAMETERS CHARACTERIZING THE SECONDARY BEAMS FROM EACH FEED IN THE REFERENCE MULTIFEED ARRAY ($\mathrm{F/D} = 0.85$)

Freq (GHz)	$G_{max}(dB)$	$G_{eoc}(dB)$	roll-off (dB)	Spill	Isolation x4	X-Pol	θ_{3dB}
9.4	43.8	39	4.8	-2.8	14.7	38.3	0.91
9.6	44.2	39.2	5	-2.6	14.5	37.4	0.89
9.8	44.5	39.3	5.2	-2.5	14.3	36.6	0.87
10	44.7	39.3	5.5	-2.5	14.4	35.2	0.86
10.2	44.9	39.3	5.7	-2.4	14.5	34.3	0.84
10.4	45.1	39.2	5.9	-2.4	14.8	33.7	0.82
10.6	45.4	39.3	6.1	-2.3	15.1	34	0.81

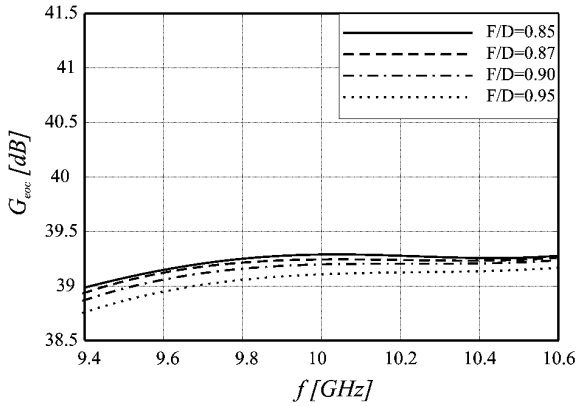

Fig. 5. Edge of coverage gain as a function of the frequency for the reference array with apertures of diameter $D_a = 1.1\lambda_0$. Different curves are referred to different F/D, given that $F = 66.66\lambda_0$.

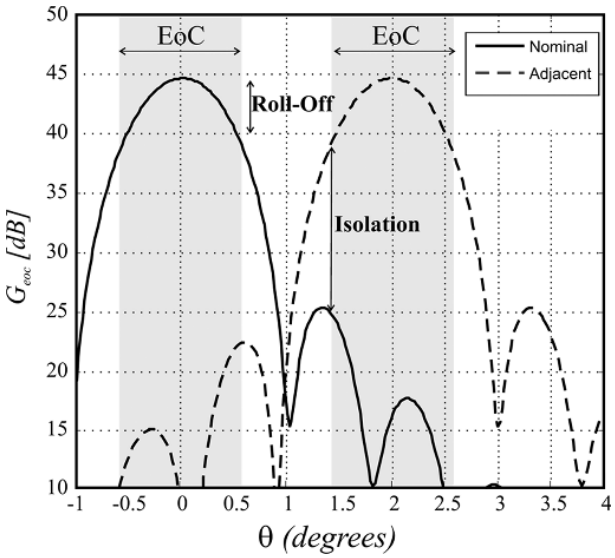

Fig. 6. Secondary pattern provided by the reflector fed by the reference array ($\mathrm{F/D} = 0.85$).

III. PATTERN SYNTHESIS BASED ON LEAKY WAVE ENHANCEMENT

In [10] a super-layer configuration, characterized by $h_1 = 0.5\lambda_0, h = 0.25\lambda_d$ and dielectric constant $\epsilon_r = 4.5$ was used for the design of a waveguide array. In that paper it was demonstrated that the mutual coupling between neighboring array elements in an hexagonal lattice configuration was dominated by the first couple of TE/TM leaky waves that were supported by the structure. When the inter-element spacing was $1.2\lambda_0$, the

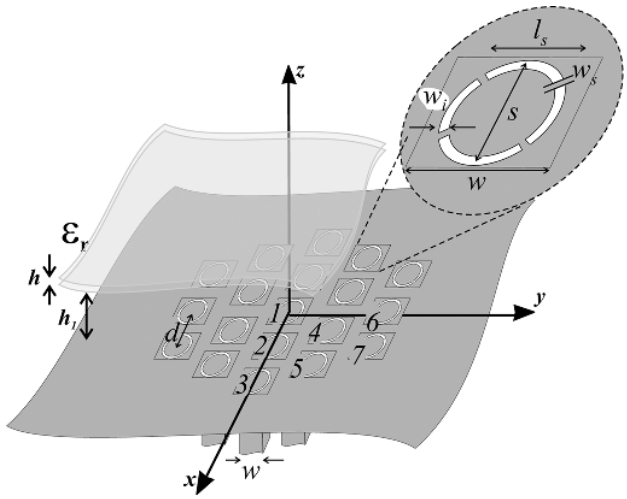

Fig. 7. Final design of the prototype waveguide array. The area of each unit cell is significantly larger than the dimension of each waveguide.

$S_{1\mathrm{j}}$ parameters, with 1 indicating the central element and j indicating any of the neighboring ones was in the order of -20 dB. When the array configuration was based on square waveguides loaded with irises, as shown in Fig. 7, the radiation patterns would turn out to be rotationally symmetric, and also minimally perturbed by the unwanted second TM mode.

The predicted patterns, at the central operating frequency, f_0 corresponding to λ_0, in four planes are reported in Fig. 8 for completeness. Both embedded and isolated patterns are shown to highlight the effects of mutual coupling on the patterns. The embedded patterns (dashed lines) are representative of a scenario in which all the waveguides surrounding the central one are terminated in matched loads: in the rest of the paper this configuration will be referred to as resistively loaded design.

The isolated patterns would instead be representative of a configuration in which the adjacent waveguides are not present and the equivalent inter-element period is $2.4\lambda_0$. In fact in that case the mutual couplings would be so low that they can be completely ignored. This configuration can be realized by introducing reactive loads in the adjacent waveguides, which synthesize equivalent short circuits. In the rest of the paper this second configuration will be referred to as reactively loaded design. Two different prototypes implementing these two designs will be discussed in the following sections.

IV. RESISTIVELY LOADED DESIGN

A prototype array was manufactured to implement the resistively loaded design at X band. An added advantage of the small

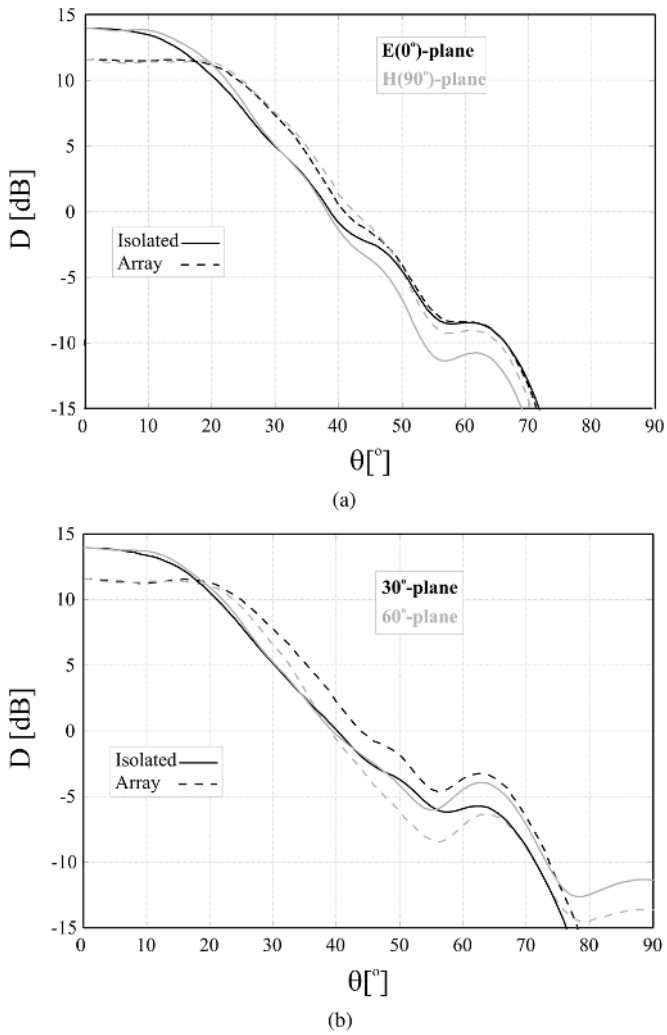

Fig. 8. Amplitude of the calculated radiation patterns. The embedded patterns (central element of the array) present more flat and wider main beams but a more rapid drop off for wider angles that would only contribute to spillover. (a) E and H planes (b) 30° and 60° planes.

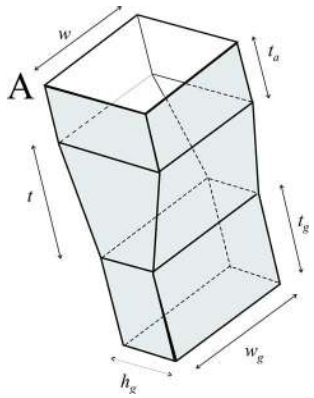

Fig. 9. Detailed view of the waveguide transitions to transform the dual polarized feed in a single WR-90 waveguide.

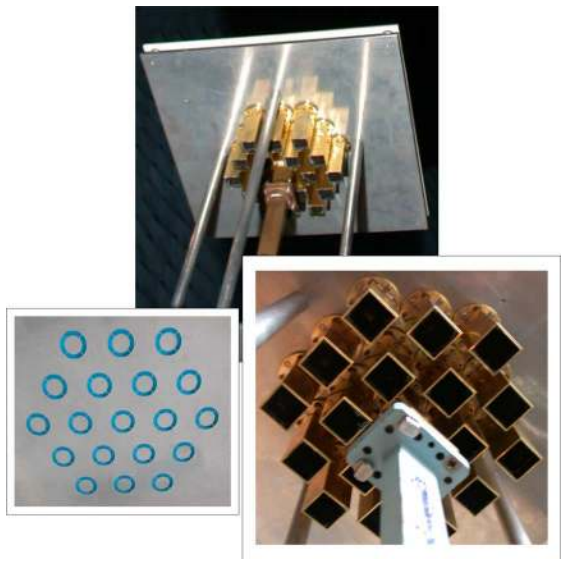

Fig. 10. Photo of the hardware demonstrator in X band. Resistively loaded design. The insets show the iris layer and the loaded waveguides.

waveguides, with respect to the larger waveguide of the reference array, is that they are easier to manufacture and connect to the common ground plane.

The central operating frequency of the prototype was chosen as $f_0 = 10$ GHz. The elements to be fed or measured are excited, in linear polarization, by a WR-90 feeding waveguides ($w_g = 22.86$ mm and $h_g = 10.16$ mm), after a smooth transition ($t = 17.3$ mm, $t_a = 10$ mm), see Fig. 9. These feeds can be mounted with two possible orientations so that also the mutual coupling between orthogonally polarized waveguides can be measured. The remaining waveguides are closed in resistive matched loads. The dielectric material has been selected to be the TMM4 from Rogers (dielectric constant of 4.5). The thickness of the slab was $h = 3.5$ mm. The remaining dimensions of the prototype are: $w = 20$ mm, $d = 36$ mm, $h_1 = 15$ mm, $w_i = 3.4$ mm, $S = 16.85$ mm, $w_s = 0.35$ mm. Both the transverse dimensions of the substrate are 360 mm. A photo of the resistively loaded prototype is shown in Fig. 10. Note that the length t_g is not important if the WR90 waveguides are closed in resistive matched loads. However this will be an important parameter in the reactively loaded prototype that will be discussed in the next section.

A. S-Parameters Measurements

The reflection coefficient of the central waveguide has been measured when all the others are loaded. The results are presented in Fig. 11. The leaky wave enhanced prototype's reflection coefficient is below -15 dB's, over a very large BW, which indicates that in this case the matching does not limit the system performances.

The mutual coupling parameters between the central waveguide and 6 neighboring ones (indicated with indices 1–7 in Fig. 7) have been measured and are shown in Fig. 12. Only the S_{12} and S_{14} couplings are significant. However they are still below -18 dB's, until 10.6 GHz

The S parameters pertinent to orthogonally polarized feeds were measured and were always lower than -30 dB's over the entire investigated BW.

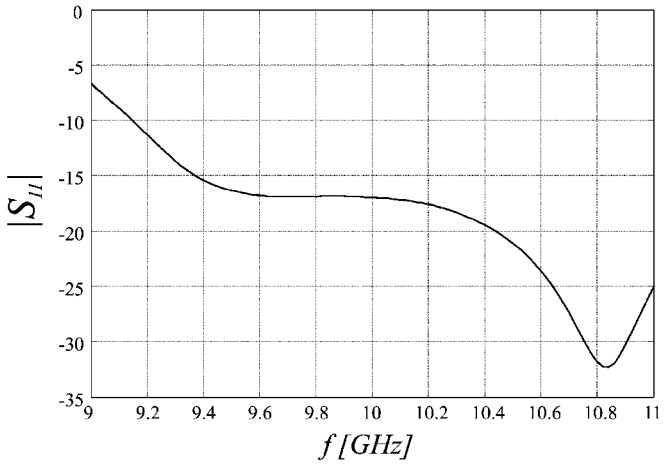

Fig. 11. Reflection coefficients of the central waveguide as a function of the frequency.

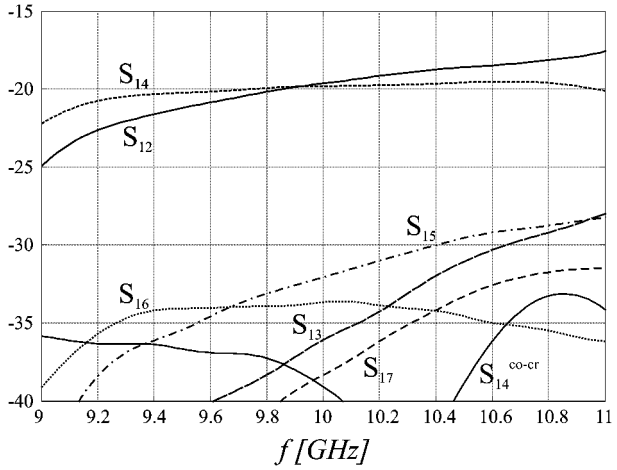

Fig. 12. S-parameters between the waveguides feeding the array when they are all mounted to obtain the same polarization.

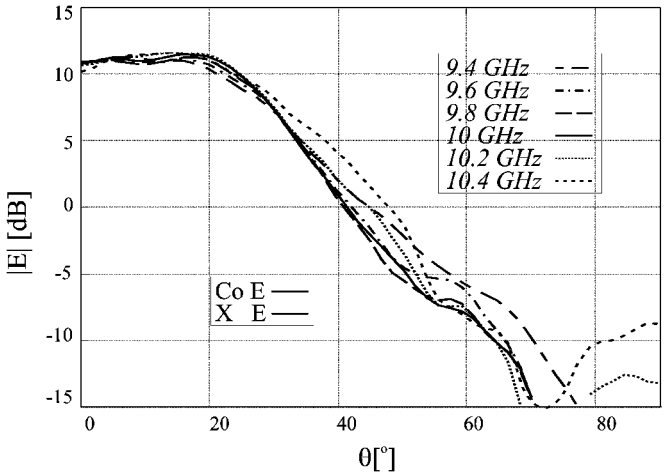

Fig. 13. Amplitude of the radiation patterns in the E-plane obtained exciting the central waveguide and loading all other waveguides with matched loads.

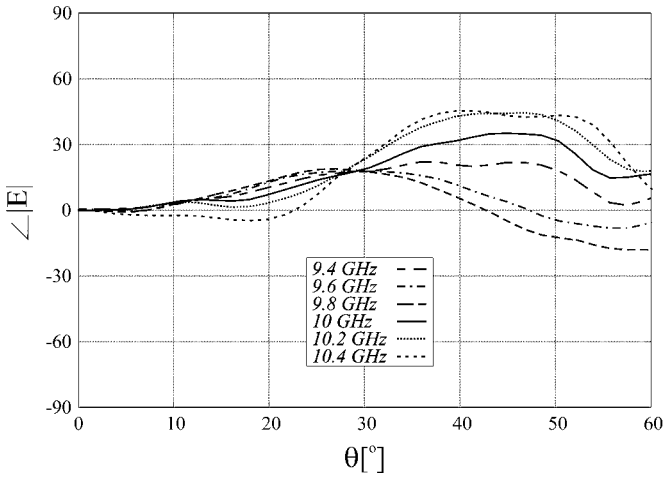

Fig. 14. Phase of the E-plane patterns as a function of the frequency.

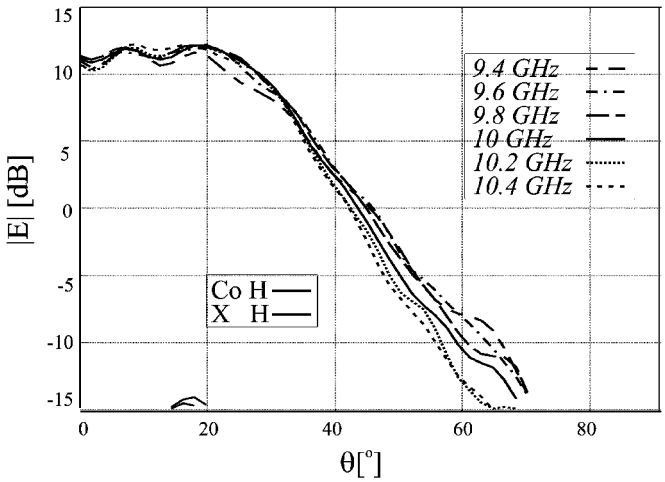

Fig. 15. Same patterns as Fig. 13 but in the H-plane.

B. Measured Patterns

The patterns from the prototype were also measured. The far field E and H plane measured embedded patterns of the central waveguide at different frequencies are shown in Fig. 13–16. The $\phi = 30$ and $\phi = 60°$ planes have also been measured. They turned out to be an average of the E and H plane patterns as expected. The measurements closely resemble the predictions, Fig. 8. The only noticeable differences are associated to amplitude ripples of less than 1 dB in the H-plane main beam. Cross polarization level are below 25 dB with respect to co-pol in all ϕ cuts. This result was to be expected due to recent findings on the polarization properties of the Green's function of a dielectric super-layer [17].

C. System Performances

The patterns were then used to calculate (using GRASP) the edge of coverage gain of a system composed by the feed array and a reflector. A parametric study of the G_{eoc}, assuming different F/D (0.85, 0.87, 0.95) and fixed focal distance $F = 2.06$ m, equivalent to that in Section II.C, is plotted in Fig. 17 as a function of the frequency. For all three F/D the gain presents a frequency dependence. Comparing it with the gain obtained

TABLE III
PARAMETERS CHARACTERIZING THE SECONDARY BEAMS FROM EACH FEED IN THE RESISTIVELY LOADED CASE

Freq (GHz)	$G_{max}(dB)$	$G_{eoc}(dB)$	roll-off (dB)	Spill	Isolation	X-Pol	θ_{3dB}
9.4	44.7	39.8	4.9	-2	13.6	42.9	0.91
9.6	45.2	40	5.2	-1.8	12.9	43.8	0.88
9.8	45.7	40.2	5.4	-1.5	12.8	43	0.86
10	46	40.4	5.6	-1.3	13	41.4	0.85
10.2	46.3	40.4	5.8	-1.2	13.4	40.4	0.83
10.4	46.3	40.3	6	-1.3	14.3	37.5	0.82
10.6	46.1	39.9	6.3	-1.7	15.7	34.3	0.81

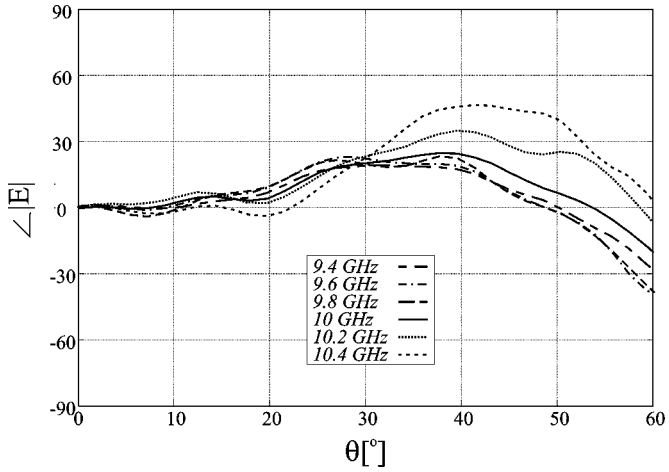

Fig. 16. Phase of the H-plane patterns as a function of the frequency.

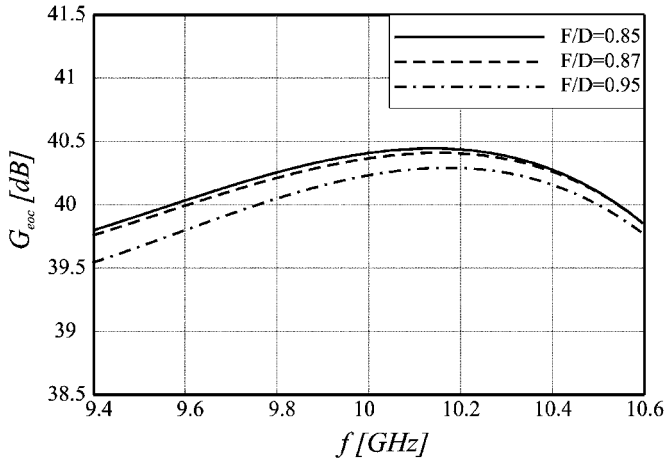

Fig. 17. Edge of coverage gain calculated from the leaky wave feeds, in the resistively loaded case. The Curves are plotted as a function of the frequency and parameterized for different F/D ratios.

using the reference array it is apparent that there is a significant improvement that can be as high as 1.2 dB for $F/D = 0.85$.

In Table III the most significant system parameters for this resistively loaded case are summarized, assuming $\mathrm{F/D} = 0.85$.

When evaluating the system performances one should take into account that part of the available power launched by the feeds is coupled in the 6 neighboring waveguides, as anticipated in [10]. The pertinent actual values of the losses as a function of the frequency have been calculated using the measured mutual couplings. They are in the order of 0.25 dBs. The losses

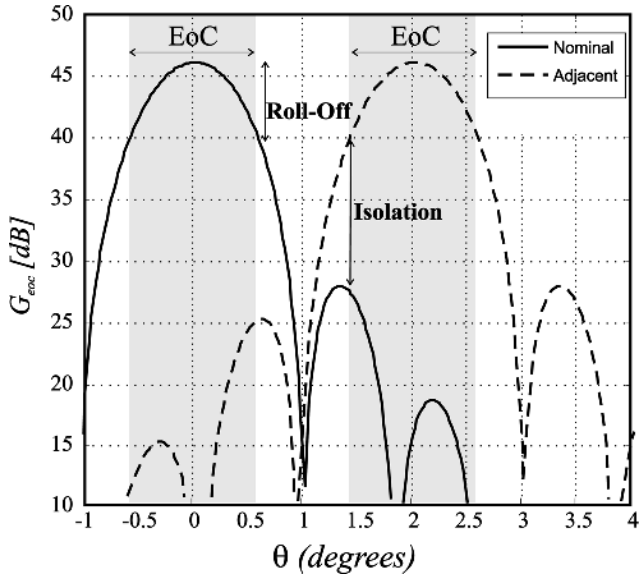

Fig. 18. Secondary pattern after the reflector in the E-plane calculated at frequency f = 10 Ghz using as feed array patterns those from the measured leaky wave feed array, $F/D = 0.85$.

have then been subtracted from the edge of coverage gains obtained using the leaky wave enhanced feed (resistively loaded case). The maximum edge of coverage gains achieved for both the reference array and the enhanced feed with $F/D = 0.85$ are compared in Fig. 19. The secondary patterns, for $\mathrm{F/D} = 0.85$ are shown in Fig. 18, at the central frequency (10 GHz), including the isolation to an adjacent pattern in a 4x frequency reuse scheme. Here the patterns associated to the two feed arrays are very similar but the leaky wave enhanced feeds provide simply higher gain values due to the fact that the power saved from spillover is radiated. It is apparent that the increase of the gain at the edge of coverage with respect to the free space case is essentially the same as that observed at broadside. Thus the leaky wave enhanced feed is more efficient in general and not only at the edge of coverage.

To summarize the results in Fig. 19 show that, even in the presence of resistively loaded neighboring waveguides, over a band width of about 12%, a minimum increase of the EoC gain of 0.6 dB can be observed. This increase becomes 0.8 dB if the band is restricted to 6%.

V. REACTIVELY LOADED DESIGN

The system performance enhancements observed in the resistively loaded array prototype were encouraging, but in order to obtain a higher increase of the EoC gain, a reactively loaded array prototype was manufactured. In this case it was assumed

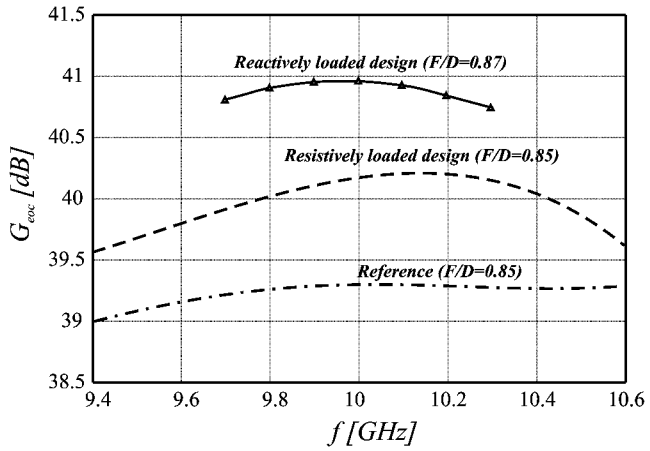

Fig. 19. Maximum $G_{\rm eoc}$ obtained using the the leaky wave feeds and the standard waveguide array. In the reference and the resistively loaded cases the optimal F/D was 0.85 while in the reactively loaded case the optimal F/D is 0.87. Note that this gain also includes the degradation of performances due to power loss in the matched loads due to mutual coupling in the six neighboring waveguides.

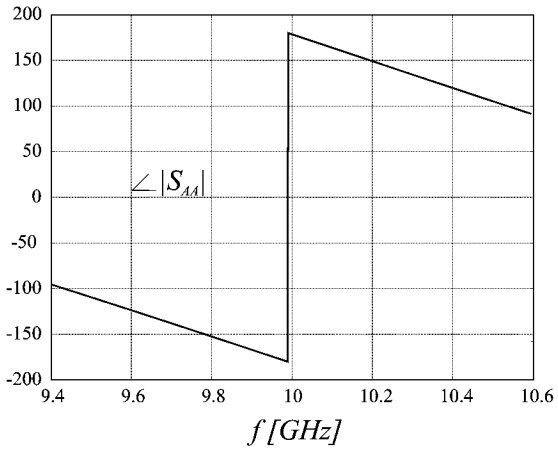

Fig. 20. Phase of the S_{AA} parameter of the feed transition shown in Fig. 9.

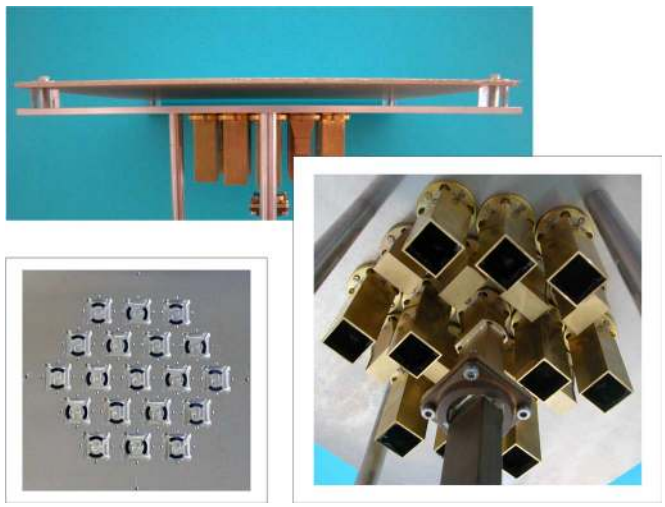

Fig. 21. Photo of the hardware demonstrator in X band. Reactively loaded design. The insets show the iris layer and the loaded waveguides.

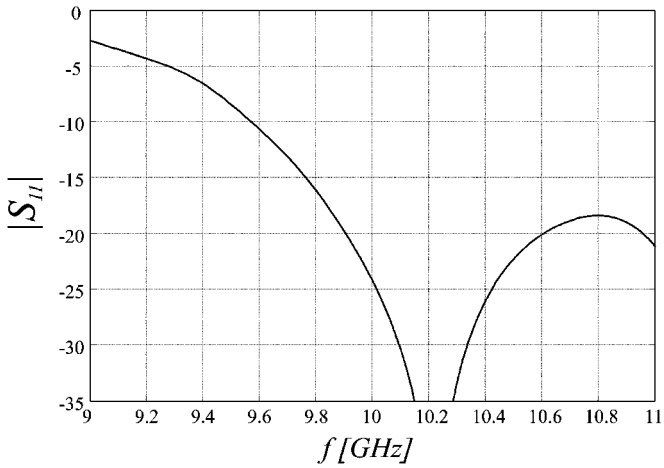

Fig. 22. Reflection coefficients of the central waveguide in the reactively loaded design.

that 4x re-use scheme was realized using two frequency bands (27.5–27.75 GHz and 28.25–28.5 GHz) and two linear polarizations to obtain a 4x frequency/polarization reuse scheme. The implementation of interleaved beams and of single aperture corresponding focal plane array is based on the same scheme described in Fig. 2. However in this case the correspondence between channel frequency and polarization was the following: $I \rightarrow co/f_1; II \rightarrow co/f_2; III \rightarrow cx/f_1; IV \rightarrow cx/f_2$

The reactively loaded prototype is very similar to the resistively loaded prototype. It is scaled to operate in the X band. The implementation of a linear polarization is simply obtained by short circuiting one of the pairs of irises in each element. The implementation of frequency selectivity is obtained loading the waveguides with two different filters which operate in the lower and the higher reflection bands respectively. The amplitudes of the S_{ii} parameters can be kept below -25 dB in the pass band and essentially 0 dB in the rejection band. The phase of the reflection at the filter cross section can be made almost constant, varying less than 15° in the rejection band. For budget reasons it was not possible to manufacture the filters. However, thanks to the smooth behavior as a function of the frequency of the phase of the reflection coefficient, the reactive load can be represented by a piece of waveguide loaded at a certain distance ($t_g = 15$ mm) by a real short circuit. The distance of the reflection plane from the aperture is tuned to achieve an effective short circuit at the aperture. The effective geometry manufactured to simulate the waveguides terminated in rejecting filters is the one shown in Fig. 9. The simulated phase of the $S_{\rm AA}$ parameter as seen from plane A is also reported in Fig. 20. It varies less than 40° degrees over the rejection BW.

The iris has been fine tuned in order to obtain the proper matching. In this case the iris parameters are: $S = 16.7$ mm, $w_i = 3$ mm and the slot edges are increased from an angle relative to the axis of 45° to an angle of 47.3°. The prototype for this reactively loaded design is shown in Fig. 21.

The measured S_{11} of the central element of the array in the presence of the reactive loading of the neighboring waveguides is presented in Fig. 22.

The radiation patterns have also been measured and they are shown in Fig. 23–26. The patterns obtained with these reactive

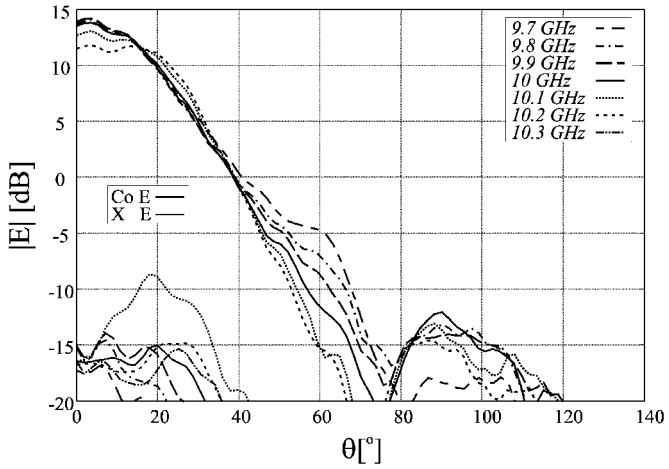

Fig. 23. Amplitude of the radiation patterns in the E-plane, reactively loaded design. The patterns are shown for different frequencies in the investigated range.

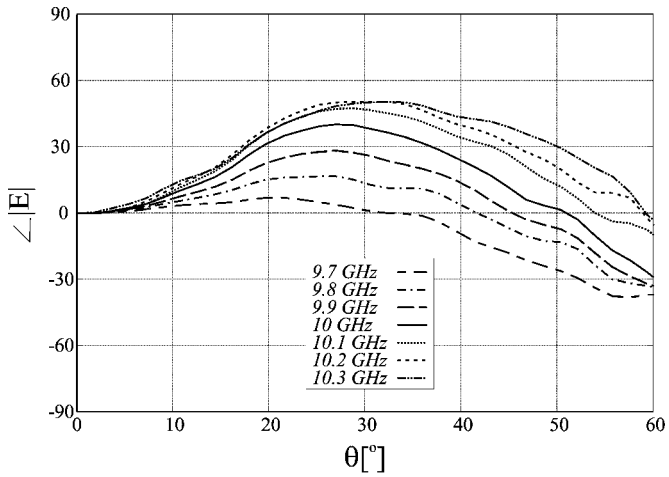

Fig. 24. Phase of the E-plane patterns as a function of the frequency, reactively loaded design.

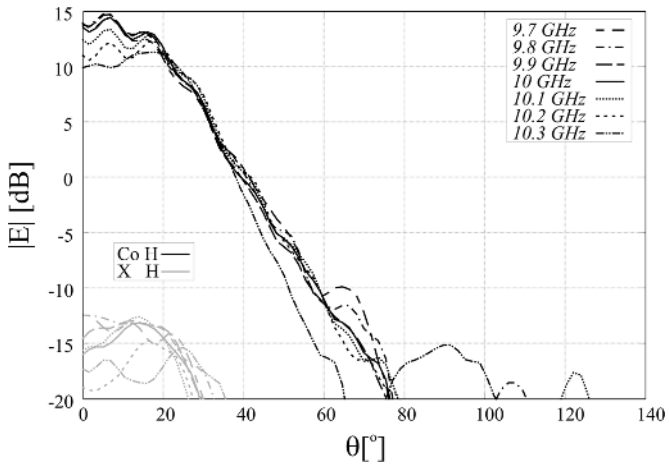

Fig. 25. Same patterns as Fig. 23 but in the H-plane.

loading are essentially the same as the isolated ones in Fig. 8. Some amplitude oscillations (of amplitude lower than 1 dB) can be observed in the main beam, however these differences turn out to be not significant in terms of the performance evaluation that follow in the next section.

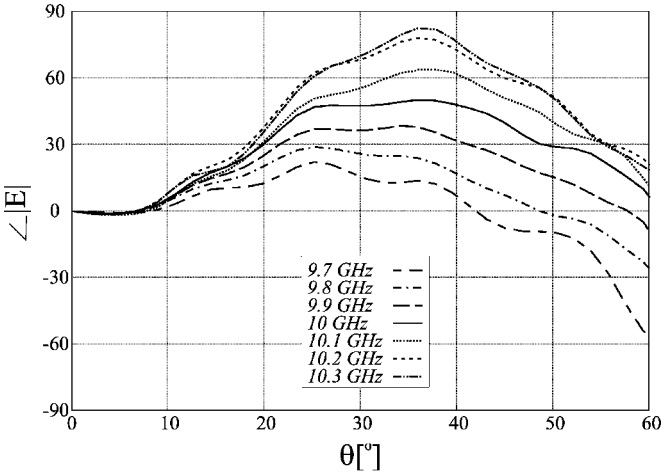

Fig. 26. Phase of the H-plane patterns as a function of the frequency.

A. System Performances

These feed patterns were then used to find the optimum EoC gain of a system composed by the feed array and the same Gregorian reflector system as for the other feeds. The optimum F/D was 0.87 and the G_{eoc} is plotted in Fig. 27 as a function of the frequency.

The gain shows stronger frequency dependence than in the other cases, due to the path length for the signal reflected in the filters, simulated in the adjacent feeds. In this case the obtained gain is significantly improved both with respect to the free space case and the resistively loaded design. In Table IV the most significant system parameters for the reactively loaded case are summarized, considering $\mathrm{F/D} = 0.87$.

The maximum increase in edge of coverage gain in the leaky wave enhanced feed configuration is as high as 1.7 dB. Over a 6% bandwidth the EoC gain is increased by 1.3 dB. Fig. 28 shows the secondary patterns with EoC limits indicated. Comparing the secondary beams of this reactively loaded design (Fig. 28) with the ones from the resistively loaded ones (Fig. 18) one can observe larger secondary beams due to a bigger aperture taper. This leads to smaller roll-off which is the second cause of EoC enhancement, after the reduced spillover. In this case the loss due to coupling to the neighboring feeds is negligible since the amplitude of the relevant S12 is lower than -35 dB. Also the adjacent beam with same frequency and polarization is shown to highlight the beam isolation, which is in the range 12 to 18 dB. Larger improvements in terms of edge of coverage gain could have been obtained, but at the expense of bandwidth.

VI. Relation to Stein's Theorem

The ruling theorem that is usually mentioned when dealing with multibeam antenna systems was formulated by Stein in [18]. Simply stated, it says that whenever an antenna presents multiple beams, the mutual coupling between the different beams limits the efficiency of the system. The mutual coupling between the beams can be quantified by calculating the S_{ij} between beam i and j either in free space or, equivalently, at feed level. A high mutual coupling implies high losses because part of the power radiated by feed j is lost in the load of feed i. If the feeds are located too close one to the other the mutual coupling grows and so do the losses. For the specific case

TABLE IV
PARAMETERS CHARACTERIZING THE SECONDARY BEAMS FROM EACH FEED IN THE REACTIVELY LOADED CASE, F/D = 0.87

Freq (GHz)	$G_{max}(dB)$	$G_{eoc}(dB)$	roll-off (dB)	Spill	Isolation	X-Pol	θ_{3dB}
9.7	44.9	40.7	4.3	-1.2	18.3	33	0.97
9.8	45.3	40.8	4.4	-1.	18.1	34.	0.96
9.9	45.6	40.9	4.6	-0.9	16.9	34	0.94
10	45.9	41.	4.9	-0.9	15.1	35	0.91
10.1	46.1	40.9	5.2	-0.9	13.4	35	0.88
10.2	46.3	40.7	5.6	-0.9	12.1	37	0.85
10.3	46.4	39.5	5.8	-1.	11.4	42	0.82

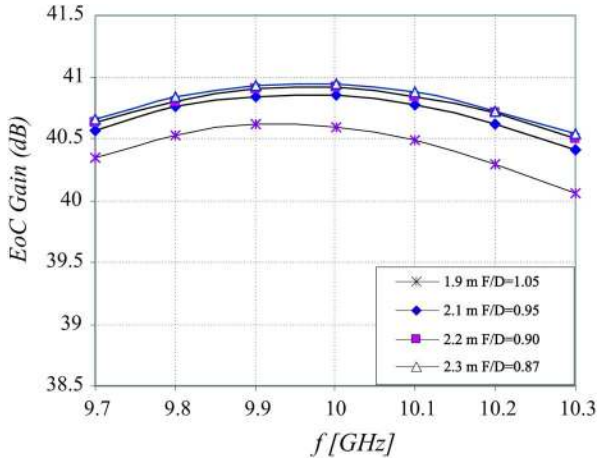

Fig. 27. Edge of coverage gain calculated from the leaky wave feeds, in the reactively loaded design. The curves are plotted as a function of the frequency and parametric for different F/D ratios.

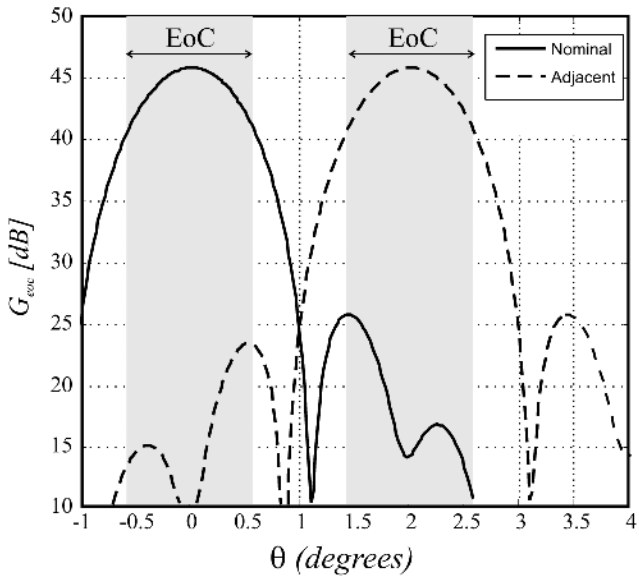

Fig. 28. Main secondary pattern calculated at frequency f = 10 GHz using as feed patterns those measured from the prototype with reactively loaded neighboring waveguide, $F/D = 0.87$.

of multifeed imaging [19] presented an in depth study of the maximum realizable secondary aperture efficiencies. There it has been shown that packing the feed elements together too much diminishes the broadside gain of the primary pattern of each of the feeds. However in [19] all feeds considered were characterized by patterns of the type $\cos^q(\theta)$. The efficiency of circular reflectors with F/D's in the order of unity was shown to be limited to about 55%.

In the present paper, the finding of the Johansson paper are essentially those represented by the reference configuration. Thus, in this paper, the comparison with the reference case could be considered as a comparison with the findings of [19]. The resistively loaded imaging configuration of Section IV shows a higher efficiency by about 15%. This finding explicitly shows that the results of [19] only constitute a upper boundary if the shape of the radiated beam obeys a $\cos^q(\theta)$ type of rule. There is no contradiction of Stein's limit since there are no greater broad side gains of the primary patterns. The rectangular primary beam shapes, that can be achieved via the leaky wave super-layers, lead to the higher primary beam efficiency, which in turn leads to a more efficient use of the reflector. This finding can be useful in those scenarios in which the attention is not necessarily to the edge of coverage but on the maximum amount of power radiated in a beam.

On the contrary the finding of the reactively loaded scenario, Section V do not imply any further improvement of the system efficiency with respect to the findings in [19]. In fact the overlap between different feeds is not really occurring. The neighboring feeds in the reactively loaded configurations are operated orthogonally, either on a different frequency or on a different polarization.

VII. CONCLUSION

A novel strategy has been presented to design multibeam reflector antenna system relaxing the conflicting requirements on the compactness of the arrays and the directivity of the feed elements. The key to improved pattern performances is the excitation of a couple of TE/TM leaky waves. They are excited by simply covering the focal plane array with a single thin dielectric layer and tuning the array design to maximize their positive effect. Taking as application scenario a telecom down-link in Ka band with x4 re-use scheme, two different designs in which the driver was edge of coverage gain have been thoroughly investigated. In the first design, the adjacent waveguides were terminated in resistive matched loads. In this case the shape of the secondary patterns remains essentially the same as those associated to the reference arrays in free space and a power enhancement can be observed at the edge of coverage thanks to the reduction of spillover with respect to a reference array. In this scenario the increase of the edge of coverage gain, $G_{\rm eoc}$, was demonstrated to be larger than than 0.6 dB over a 12% BW. Apart from the mentioned telecom scenario any application in which beam efficiency is the goal could benefit from the resistively loaded designs.

In the second design the adjacent waveguide were terminated in reactive loads realized via filters that would implement equivalent short circuits at the apertures. Here an edge of coverage increase of up to 1.3 dB was demonstrated over a BW of 6%. The

better performance, with respect to the resistively loaded design, is due to higher directivity from each feed which focuses the radiated beams in the central part of the reflector. Consequently the secondary beams are broader lowering the roll-off. In this reactively loaded design, a relaxation of the BW requirements would lead to better scanning performances for systems using larger equivalent F/D ratios. This further steps probably would require higher level trade offs in the system but the single reflector option for multibeam satellite telecommunication scenarios seems a viable option.

APPENDIX
FOCAL PLANE ARRAY FOR A FULLY SAMPLED FIELD OF VIEW

Three basic design parameters, with their approximate relationships, seem to be defining the performances of the imaging system: the beam separation $\Delta\theta$, the reflector diameter, D, and the focal distance, F (see Fig. 1).

If the system needs to make use of the entire available field of view, the half power beam width will be designed to be equal to the beam separations: $(\theta_{3\mathrm{dB}} \approx \Delta\theta)$. Since $\theta_{3\mathrm{dB}}$ can be approximated as a function of the reflector diameter as $\theta_{3\mathrm{dB}} \approx \lambda_0/D$ it follows that the beam separation is linked to the antenna diameter by: $\Delta\theta \approx \lambda_0/D$

F, relates the beam separation to the separation, d, in the focal plane between the different array elements: $\Delta\theta \approx d/F$, is a simplified formula provided in [12] for small values of $\Delta\theta$. From the use of these simple relationships between the previous three parameters follows the key imaging array law that estimates the separation between the different feeds in order to achieve a fully sampled sky:

$$d = F \cdot \Delta\theta = D \cdot (F/D)\lambda_0/D \approx (F/D)\lambda_0. \qquad (2)$$

ACKNOWLEDGMENT

This work was performed under contract with the European Space Agency (ESA): Photonic Bandgap Terminal Antennas (Contract No. 18953/05/NL/JA). Thanks are expressed to Cyril Mangenot, Head of the Antenna Section at ESA-ESTEC, for stimulating discussions and to Pablo Sarassa for providing information on realistic filtering functions.

REFERENCES

[1] S. K. Rao, "Design and analysis of multiple-beam reflector," *IEEE Antennas Propag. Mag.*, vol. 41, pp. 53–59, Aug. 1999.
[2] G. V. Trentini, "Partially reflecting sheet arrays," *IEEE Trans. Antennas Propag.*, vol. 4, no. 4, pp. 666–671, Oct. 1956.
[3] S. I. Khurein Castiglioni, G. Toso, and C. Mangenot, "Multi-beam antenna based on a single aperture using overlapped feeds," presented at the 13th JINA Int. Symp. on Antennas, Nice, France, Nov. 8–10, 2004.
[4] C. Cheype, C. Serier, M. Thevenot, T. Monediere, A. Reineix, and B. Jecko, "An electromagnetic bandgap resonator antenna," *IEEE Trans. Antennas Propag.*, vol. 50, no. 9, pp. 1285–1290, Sep. 2002.
[5] Y. J. Lee, J. Yeo, R. Mittra, and W. S. Park, "Application of electromagnetic bandgap superstrates with controllable defects for a class of patch antennas as spatial angular filters," *IEEE Trans. Antennas Propag.*, vol. 53, no. 1, pp. 224–235, Jan. 2005.
[6] N. Guerin, S. Enoch, G. Tayeb, P. Sabouroux, P. Vincent, and H. Legay, "A metallic Fabry-Perot directive antenna," *IEEE Trans. Antennas Propag.*, vol. 54, no. 1, pp. 220–224, Jan. 2006.
[7] D. R. Jackson, A. A. Oliner, and I. P. Antonio, "Leaky wave propagation and radiation for a narrow-beam multiple layer dielectric structure," *IEEE Trans. Antennas Propag.*, vol. 41, no. 3, pp. 344–348, Mar. 1993.
[8] R. Gardelli, M. Albani, and F. Capolino, "Array thinning by using antennas in a Fabry-Perot cavity for gain enhancement," *IEEE Trans. Antennas Propag.*, vol. 54, no. 7, pp. 1979–1990, Jul. 2006.
[9] A. Neto, N. Llombart, G. Gerini, M. Bonnedal, and P. de Maagt, "EBG enhanced feeds for the improvement of the aperture efficiency of reflector antennas," *IEEE Trans. Antennas Propag.*, vol. 55, no. 8, Aug. 2007.
[10] N. Llombart, A. Neto, G. Gerini, M. Bonnedal, and P. De Maagt, "Impact of mutual coupling in leaky wave enhanced imaging arrays," *IEEE Trans. Antennas Propag.*, vol. 56, pp. 1201–1206, Apr. 2008.
[11] C. A. Balanis, *Antenna Theory: Analysis and Design*, 3rd ed. New York: Wiley Interscience, 2005.
[12] Y. Rahmat-Samii, "Reflector Antennas," in *Antenna Handbook*, Y. T. Lo and S. W. Lee, Eds. New York: Van Nostrand Reinhold , 1988.
[13] Y. Mizugutch and H. Yokoi, *Trans. IECE Jpn*, pp. 58–3, 1975, 2.
[14] K. Pontoppidan, TICRA Engineering Consultants, Copenhagen, Denmark, *Technical Description GRASP9,* Feb. 2005.
[15] CST Microwave Studio, Darmstadt, Germany, *User Manual Version 5.0.*
[16] M. Qiu and G. Eleftheriades, "A reduced surface-wave twin arc-slot antenna element on electrically thick substrates," *IEEE Microw. Wireless Compon. Lett.*, pp. 459–461, Nov. 2001.
[17] A. Polemi and S. Maci, "On the polarization properties of a dielectric leaky wave antenna," *IEEE Antennas Wireless Propag. Lett.*, vol. 5, pp. 306–310, 2006.
[18] S. Stein, "On cross coupling in multi beam antennas," *IRE Trans. Antennas Propag.*, vol. AP 10, pp. 548–557, Sep. 1962.
[19] K. S. Yngvesson, J. F. Johansson, Y. Rhamat-Samii, and Y. S. Kim;, "Realizable feed element patterns and optimum aperture efficiency in multi beam antenna systems," *IEEE Trans. Antennas Propag.*, vol. 36, no. 11, pp. 1637–1641, Nov. 1988.

Nuria Llombart (S'06–M'07) received the Ingeniero de Telecomunicaciόon degree and the Ph.D. degree from the Universidad Politécnica de Valencia, Spain, in 2002 and 2006, respectively.

During her Master's degree studies she spent one year at the Friedrich-Alexander University of Erlangen-Nuremberg, Germany, and worked at the Fraunhofer Institute for Integrated Circuits, Erlangen, Germany. From 2002 until 2007, she was with the Antenna Unit, Defence, Security and Safety Institute, Netherlands Organization of Applied Scientific Research (TNO), The Hague, The Netherlands, working as Ph.D. student and afterwards as researcher. Currently she is a Postdoctoral Fellow at the California Institute of Technology, Pasadena, working for the S.W.A.T. group of the Jet Propulsion Laboratory. Her research interests include the analysis and design of printed array antennas, EBG structures, and reflector antennas.

Dr. Llombart was a co-recipient of the 2008 H. A. Wheeler Applications Prize Paper Award from the IEEE Antennas and Propagation Society.

Andrea Neto (M'00) received the Laurea degree (*summa cum laude*) in electronic engineering from the University of Florence, Florence, Italy, in 1994 and the Ph.D. degree in electromagnetics from the University of Siena, Siena, Italy, in 2000.

Part of his Ph.D. was developed at the European Space Agency Research and Technology Center, Noordwijk, The Netherlands, where he has been working for the antenna section for over two years. From 2000 to 2001, he was a Postdoctoral Researcher at California Institute of Technology, Pasadena, working for the Sub-mm wave Advanced Technology Group. Since 2002, he is a Senior Antenna Scientist at TNO Defence, Security and Safety, Den Haag, The Netherlands. He is the coauthor of five patent applications and over 150 contributions to peer reviewed journals and international conference

proceedings. Over 20 of these papers have appeared in IEEE TRANSACTIONS. His research interests are in the analysis and design of antennas, with emphasis on arrays, dielectric lens antennas, wide band antennas and EBG structures.

Dr. Neto was a co-recipient of the 2008 H. A. Wheeler Applications Prize Paper Award from the IEEE Antennas and Propagation Society.

Giampiero Gerini (M'92–SM'08) received the M.S. degree (*summa cum laude*) and the Ph.D. in electronic engineering from the University of Ancona, Ancona, Italy, in 1988 and 1992. respectively.

From 1994 to 1997, he was a Research Fellow at the European Space Research and Technology Centre (ESA-ESTEC), Nooordwijk, The Netherlands, where he joined the Radio Frequency System Division. Since 1997, he has been with the Netherlands Organization of Applied Scientific Research (TNO), The Hague, The Netherlands. At TNO Defence, Security and Safety, he is currently chief senior scientist of the Antenna Unit in the Transceivers and Real-time Signal Processing Department. His main research interests are phased array antennas, frequency selective surfaces and integrated front-ends.

Dr. Gerini was a co-recipient of the 2008 H. A. Wheeler Applications Prize Paper Award from the IEEE Antennas and Propagation Society.

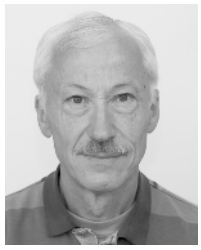

Magnus Bonnedal (M'74) received the M.Sc. degree in electrical engineering and the Ph.D. degree in plasma physics from Chalmers University of Technology, Gothenburg, Sweden, in 1972 and 1979, respectively.

Since then he has been working at Ericsson and Saab Space, Goteborg, Sweden, with development of arrays, reflector antennas and feed systems in communication and earth observation applications. Currently, he is primarily engaged in the development of navigation receivers for satellite precise orbit determination and earth observation.

Peter de Maagt (S'88–M'88–SM'02–F'07) was born in Pauluspolder, The Netherlands, in 1964. He received the M.Sc. and Ph.D. degrees from Eindhoven University of Technology, Eindhoven, The Netherlands, in 1988 and 1992, respectively, both in electrical engineering.

He is currently with the European Space Research and Technology Centre (ESTEC), European Space Agency, Noordwijk, The Netherlands. His research interests are in the area of millimeter and submillimeter-wave reflector and planar integrated antennas, quasi-optics, electromagnetic bandgap antennas, and millimeter- and submillimeter-wave components.

Dr. de Maagt was a co-recipient of the 2001 and 2008 H. A. Wheeler Applications Prize Paper Award from the IEEE Antennas and Propagation Society. He was granted a European Space Agency Award for Innovation in 2002. He was also a co-recipient of the Loughborough Antennas and Propagation Conference (LAPC) 2006 Best Paper Award and the International Workshop on Antenna Technology (IWAT) 2007 Best Paper Award.